ASME Journal of Nuclear Engineering and Radation Science, Volume 6, Issue 2, April 2020, Article number 021201
DOI:10.1115/1.4044260

Performance Modeling and Analysis of Independent Control Strategies for Part-Load Operations and Load Rejection of a Single-Shaft Closed-Cycle Gas Turbine

Emmanuel O. Osigwe[*]
Power Propulsion Engineering Center
Cranfield University
Bedford, Bedfordshire, MK43 0AL, UK

Arnold Gad-Briggs
EGB Engineering UK, Southwell, United Kingdom
Cranfield University
Bedford, Bedfordshire, MK43 0AL, UK

Dodeye Igbong
Power Propulsion Engineering Center
Cranfield University
Bedford, Bedfordshire, MK43 0AL, UK

Theoklis Nikolaidis
Power Propulsion Engineering Center
Cranfield University
Bedford, Bedfordshire, MK43 0AL, UK

Pericles Pilidis
Power Propulsion Engineering Center
Cranfield University
Bedford, Bedfordshire, MK43 0AL, UK

Abstract

In the last few years, one considerable factor for the viability and interest in the closed-cycle gas turbine systems for nuclear or conventional power plant application is its potential to maintain high cycle performance at varying operating conditions. However, for this potential to be realised, more competitive analysis and understanding of its control strategy are importantly required. In this paper, the iterative procedure for three independent control strategies of a 40 megawatt single-shaft intercooled-recuperated closed-cycle gas turbine incorporated to a Generation IV nuclear reactor is been analysed and their performance at various operating conditions compared. The rationale behind this analysis was to explore the different control strategy and to identify potential limitations using each independent control. The inventory control strategy offered a more viable option for high efficiency at changes in ambient and part-load operations, however, operational limitations in terms of size and pressure of inventory tank, rotational speed for which the centrifugal forces acting on the blade tips could become too high, hence would affect the mechanical integrity and compressor performance. The bypass control responds rapidly to load rejection in the event of loss of grid power. And more interestingly the results showed the need for a mixed or combined control instead of a single independent technique, which is limited in practice due to operational limits.

Keywords: Nuclear Reactor, Performance Modelling, Closed-cycle gas Turbine, Energy conversion, cycle performance

1. Introduction

In retrospect, the closed-cycle gas turbine is considerably ahead of its time in terms of technology readiness since its first commercial plant was built in 1939 by Escher Wyss [1]. Ever since, there has been growing efforts in research and developments, on the improvement of existing designs, control systems and cycle performance, as well as new innovative concepts with different working fluid configurations [2]. Interestingly, the closed-cycle gas turbine offers viable prospect for stable conversion of nuclear or fossil fuels into electrical and heat energy due to (a) its easy adaptability (b) flexibility to changes in working fluid (c) high efficiency of electricity generation at part load (d) high level of availability and low maintenance cost. More so, the closed-cycle gas turbine offers potential savings in operating cost due to its ability to relatively maintain high-performance efficiency under varying operating conditions, when

compared with other advanced cycles [3,4]. However, the advantage of the later can be achieved by implementing appropriate control strategy during the operation of the power plant. Hence, the need for this paper to provide a completive understanding of the closed-cycle gas turbine controls strategies.

There are different control strategies that are applicable to the successful operations of the closed-cycle gas turbine power plant which are documented in references [1,5–9]. However, for the purpose of this study, the inventory, bypass and heat source temperature controls were considered in this paper. The goal of these control strategies implemented in the closed-cycle gas turbine system would be (a) for the power plant to quickly adjust to wide range of fluctuating load variation without significantly affecting the cycle thermal efficiency (b) for prevention of thermal shocks on plant components during critical transients, and (c) for providing automatic control manoeuvres during plant start up and shut down and (d) for operational stability of the plant to avoid eventualities. Consequently, in an attempt to understand the modelling concept and operation of the control strategies, previous work on control strategies for closed-cycle gas turbine operations was reviewed. Covert et al., [5] described the effect of three distinct control mode on the cycle performance at steady-state full and part-load operations of a helium direct-cycle nuclear gas turbine power plant. The overarching result showed that the helium inventory control maintained high cycle efficiency over other control options mentioned in their work. The work by reference [7] described other alternative control options for the safe operation of the plant in event of an abnormal shut down or system emergency. It also described the dynamic behaviour of a single-shaft closed-cycle operation using bypass control mode. Similarly, references [8,10] have investigated the operational envelope of bypass control during transients. Botha et al. [9] described load rejection control for a three-shaft closed-cycle gas turbine. In references [6,11–14], the different authors described the inventory control systems for load-following in terms of cycle performance based on the energy mix in the electricity grid as may be required by the regulators.

To this end, the aim of this paper is to present the steady-state performance modelling and analysis of selected control options for a single-shaft intercooled-recuperated closed-cycle gas turbine power plant under varying operating conditions. The control methods developed in this paper was based on parametric analysis of influencing cycle parameters like pressure ratio, heat source temperature, and mass flow on the plant performance. By manoeuvring these parameters using appropriate control logic, the plant can be regulated to match any changes in load demand or sudden requirement for idling or shutdown. This paper partly complements works of previous authors on part-load control strategies for a closed-cycle gas turbine. However, to the best of the authors' knowledge, none of the references cited so far provided a detailed description of the iterative procedure for predicting closed-cycle gas turbine performance at various off-setting conditions using the different control strategy mentioned in this paper. More so, in this paper, a pseudo-transient behaviour of the plant using by-pass control has been described.

2. Control Options

As previously mentioned, the selection of the reference plant control system followed an evaluation of several alternatives documented in [7], and reference [5] discussed the effects on the part-load performance of some of the alternative means of control. The control options presented in this paper are: Inventory control, bypass and heat source temperature control strategies.

2.1 Inventory Control Strategy (ICS)

This control option has been widely mentioned as an attractive possibility [15] because it allows the power plant to operate within a wide range of load fluctuation at a good cycle thermal efficiency. The operating concept of the control logic is for the power plant to be able to store, or save energy during off-peak periods and replenish this energy during peak load demand via inventory control system (ICS). This means that the working fluid is either extracted or injected into the power conversion system, resulting in a related change in system pressure, change in density, change in mass flow rate and, therefore, also a change in power level.

During the reference plant operations, the daily fluctuations in power demand as a result of varying operating conditions are adjusted by means of the inventory control system (ICS). The ICS comprises of the inventory control tank (ICT), and inventory control valves (ICV) as shown in Fig. 1. When reduction of shaft power is required as a result of a decrease in load demand, the ICV1 is opened so that the working fluid flows from the High-Pressure Compressor (HPC) into the ICT. The working fluid stored in the ICT(s) can be injected back into the power conversion circuit by the opening of ICV3, and ICV6 if the output power is to be increased to full capacity. When inventory control is initiated, the heat source temperature and shaft speed are controlled to remain constant.

The inventory control system is regulated based on the pressure variation between the plant cycle and the inventory tank. This variation determines the power limit and the possibility of maintaining high part-load efficiency to which inventory control is achieved. However, there are restrictions to the extent the inventory control system can maintain a high part load efficiency, which includes [16]: (a) size and pressure of the inventory storage tank, (b) shaft rotational speed effect on blade tips (c) location of inventory valves in the cycle loop (d) availability of inventory transfer compressor, and (e) cost of implementing any of the options listed.

2.2 Bypass Control Strategy (BCS)

In this case, the power level is controlled by regulating the bypass valve as shown in fig. 1. The high-pressure gas is bled off to short-circuit the gas heater (GH) and turbine to the low-pressure side of the recuperator, and, as such, the mass flow, pressure ratio and efficiency of the turbine drop, causing a decrease in the output power. The redirected flow is circulated into the compressor at an unchanged gas inventory, thus, increasing the pressure level and compressor work. The Low-Pressure Compressor (LPC) pressure decreases as the bypass valve opens. This decreases the turbine pressure ratio and adds to the reduction of the turbine power. The same effect takes place in the HPC. The cycle gas path temperatures do change, with just the thermal power input matching the deficits required to maintain the cycle temperatures at reduced mass flow through the heat source.

The advantage of this control option is that it can be initiated during rapid power changes or emergency to match the load variation. Thus, this control option is usually implemented in closed-cycle gas turbines to achieve fast control response and to prevent the shaft from over-speeding [17,18]. The cycle analysis is merely a working accounting with the full mass flow processed by the compressor and less in the heater and turbine. An ideal cycle analysis gives

$$Cycle\ thermal\ efficiency\ \eta_{th}\ (\%) = \left[1 + \frac{SP}{SP_{max}}\left(\frac{\theta_8}{\theta_2} - 1\right)\right]^{-1} \quad (1)$$

Where,

$$SP_{max} = \left(\frac{\theta_8}{\theta_2} - 1\right)(\theta_2 - 1), \qquad \theta_8 = \frac{T_8}{T_{ref}},\ \theta_2 = \frac{T_2}{T_{ref}} \tag{2}$$

Figure 3 shows the iteration modelling procedure using bypass control at a steady-state condition.

2.3 Heat Source Temperature Control (HST)

The heat source temperature refers to the reactor discharge temperature delivered to the gas turbine. Thus, the power level is altered by changing the temperature of the working fluid at the gas heater (GH) via changes in the heat source temperature. In this case, the fluid circulating inventory remains constant, and a drop in Turbine Entry Temperature (TET) causes a decrease in the components cycle temperature and pressure distribution. These changes affect the overall performance of the power plant. The HST control is an effective control for the varying operating condition, however, in reality, due to the effect of over-speed; this control is usually balanced with bypass control option. Fig. 4 describes the iteration procedure with heat source temperature control.

2.4 Combined Control Strategy

The combine control strategy utilizes integrated control actions of the options mentioned above to regulate the behaviour of the engine in order to avoid limitations in shaft speed or low cycle efficiencies. This approach consists of controllers which issue commanding signals to the control options subsystems to perform integrated control functions. The load demand acts as the primary input which determines the appropriate control subsystem to be initiated. In real time operation of any closed-cycle gas turbine power plant, either all or part of these control methods discussed is simultaneously utilized to meet diverse control requirements during operation. Hence, a combined control system is usually integrated with several subsystems to allow the interactive control action as required. For example, a combined control mode can be designed to have an inventory control for slow load moderation, a bypass control for rapid load response, shaft speed control and emergency shut-down capability, and a heat source temperature control to regulate heat source power input as required by the system as shown in fig. 1.

During this operation certain percentage of power-level change triggers the control response for load-following or load-rejection.

3. Engine System Description

A Generation IV nuclear reactor indirectly coupled with an inter-cooled recuperated (ICR) closed-cycle gas turbine configuration was used in the analysis. The main design characteristic of the ICR power plant is based on the cycle shown in Fig (1). The cycle consists of a low-pressure compressor (LPC), intercooler (IC), high-pressure compressor (HPC), a recuperator heat exchanger (RX), gas-heater (GH), turbine, a pre-cooler (PC) and the Very High-Temperature Reactor (VHTR). Both the LPC and HPC are driven on a single shaft. A summary of the plant characteristic is described in Table 1. From the diagram presented in Fig.1, the ICVs refer to the inventory control valves. The valve lift of the ICVs is actuated by an output controller, which has an input signal of the difference between the nominal and actual power output. This variation triggers the opening and closing of the ICVs. The bypass valve opens when the

bypass control is initiated during a sudden drop in load demand as may be required during the plant operation. In most operations, this is usually initiated at >10% sudden drop in the gas turbine output power. Further explanation of the valve operation is discussed in reference [1].

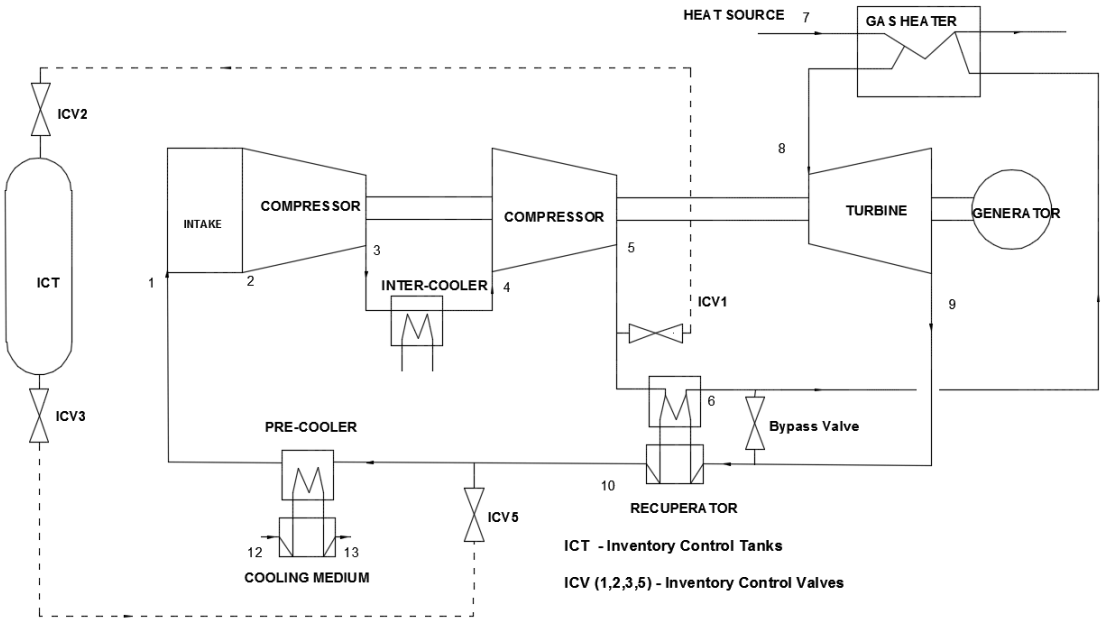

Figure 1: Scheme of Reference Plant Circuit with Different Control Options

Table 1: Summary of Power Plant Description

Description	Unit
Heat Source Temp. (K)	1100
LPC Pressure ratio	1.65
LPC Inlet Pressure (kPa)	830
LPC Inlet Temperature (K)	290
HPC Pressure ratio	2.40
LPC& HPC efficiency (%)	86
Turbine efficiency (%)	90
Flow rate at LPC (kg/s)	230
Plant Thermal Efficiency (%)	41.2
IC effectiveness (%)	90
RX & GH effectiveness (%)	90
Rated power (MW)	40.8
Working Fluid	Air

4. Method of Analysis and Equations

The reference plant steady state performance presented herein was modelled with an in-house computer simulation code developed by the authors of this paper for closed cycle performance simulations [19]. The simulation tool has two basic modes of operations, design and off-design point. A design point calculation is used to obtain a solution at just one operating point; this may

be done with or without the component maps. The off-design procedure was analysed as a function of design point performance, plant control settings and a wide array of operating conditions.

To simplify the description of the simulation code, an iterative procedure for calculating the behaviour of the closed-cycle gas turbines using the selected control options is given and applied on single-shaft power plants, namely: change of inventory, actuating a bypass and heat source temperature control. The working fluid thermodynamic and heat transfer properties were provided by a series of subroutines which computes the enthalpy, viscosity, gamma, specific gas constants, and conductivity as functions of temperature and pressure. Components and duct pressure drops were computed as a function of design point pressure drops by ratios of appropriate functions of the fluid properties and mass flow rate.

In determining the design point condition, the compressor pressure ratios, inlet temperature and pressure, turbomachinery efficiency and heat source temperature were considered as independent variables. The design point operations utilize a common input for all control strategies and produce identical performance data which are fed into the off-design calculations for the different control strategy initiated. When the calculations of the thermodynamic state quantities of the reference plant at design point are concluded, the non-dimensional characteristics are then evaluated [20]. These non-dimensional groups are then required as input data in the off-design calculation to scale the available characteristics curve of the reference plant. The pressure losses and mass leakage at design point are accounted for in the model. Model descriptions of each component that constitute the overall performance of a closed-cycle gas turbine are described as follow:

Turbo-set: This includes the compressor and the turbine. The behaviour of the turbo-set is described with dimensionless parameters such as corrected mass flow, corrected speed, pressure ratio, component efficiencies and work functions. These parameters are plotted on graphs with lines of pressure ratio against the corrected mass flow for different corrected speed lines and contour lines of constant efficiency. It is essential when expressing these parameters that the properties of the working fluid are taken into consideration, which is expressed as:

$$CMF = \left(\frac{W\sqrt{\theta}}{\delta} \times \sqrt{\frac{R}{\gamma}}\right), \qquad CS = \left(\frac{N}{\sqrt{\theta R\gamma}}\right), \qquad CH = \left(\frac{\Delta H}{\sqrt{\theta R\gamma}}\right) \tag{3}$$

Where,

$$\theta = \frac{T}{T_{ref}}, and\ \delta = \frac{P}{P_{ref}}$$

The compressor exit temperature (℃) is given by the expression

$$T_{C_{out}} = T_{c_{in}} + \frac{T_{c_{in}}}{\eta_c}\left[\left(\frac{P_{c_{out}}}{P_{c_{in}}}\right)^{\left(\frac{\gamma-1}{\gamma}\right)} - 1\right] \tag{4}$$

The compressor exit pressure is derived from the given pressure ratio as:

$$PR_c = \frac{P_{c_{out}}}{P_{c_{in}}} = f\ (CMF, CS) \tag{5}$$

The compressor work (W), is a product of the mass flow, specific heat capacity at constant pressure and the overall temperature rise in the compressor. This is given as:

$$CW = WC_{P_{out}} T_{c_{out}} - WC_{P_{in}} T_{c_{in}} \tag{6}$$

Similarly, the turbine exit temperature (°C) is given by:

$$T_{t_{out}} = T_{t_{in}} - T_{t_{in}} \eta_t \left[1 - \left(\frac{P_{t_{out}}}{P_{t_{in}}}\right)^{\left(\frac{\gamma-1}{\gamma}\right)}\right] \tag{7}$$

And turbine work (W) is expressed as:

$$TW = WC_{P_{out}} T_{t_{out}} - WC_{P_{in}} T_{t_{in}} \tag{8}$$

The turbine discharge pressure ratio is calculated using Eq (9)

$$PR_t = \frac{P_{t_{out}}}{P_{t_{in}}} = PR_c \left[\frac{\sum(1 - \Delta P)_{HPS}}{\sum(1 + \Delta P)_{LPS}}\right] \tag{9}$$

Heat Exchangers: The heat exchangers which include the recuperator, gas heater and pre-cooler were modelled using the effectiveness-number of transfer function (ε-NTU) method and a counter-flow shell and tube configuration was assumed. The ε-NTU method was used since the inlet condition (temperature and pressure) of the fluid stream can be easily obtained and simplifies the iteration involved in predicting the performance of the flow arrangement. This method is fully described in references [2,21,22]. The approach also assumes that the heat exchanger effectiveness is known and the pressure losses are given.
Therefore, the effectiveness of the heat exchanger is the ratio of the actual heat transfer rate to the thermodynamically limited maximum heat transfer rate available in a counter flow arrangement.

$$\varepsilon = \frac{Q_{actual}}{Q_{max}} \tag{10}$$

$$= \frac{C_{hot}(T_{hotin} - T_{hotout})}{C_{min}\ (T_{hotin} - T_{coldin})}$$

$$= \frac{C_{cold}(T_{coldout} - T_{coldin})}{C_{min}\ (T_{hotin} - T_{coldin})}$$

Where,

$$C_{min} = \begin{cases} C_{hot}\ for\ C_{hot} < C_{cold} \\ C_{cold}\ for\ C_{cold} < C_{hot} \end{cases} \quad (11)$$

$$C_{hot} = (WC_P) hot\ fluid\ Stream$$

$$C_{cold} = (WC_P) cold\ fluid\ Stream$$

For counter flow shell and tube heat exchangers, number of transfer unit (NTU) is given by:

$$NTU = \frac{LOG_e\left[\frac{2 - \varepsilon(1 + C^* - \eta_{Hex}}{2 - \varepsilon(1 + C^* + \eta_{Hex}}\right]}{\eta_{Hex}} \quad (12)$$

Where,

$$C^* = Capacity\ rate\ ratio = \frac{C_{min}}{C_{max}} \quad (13)$$

$$\eta_{Hex} = (C^{*2} + 1)^{0.5} \quad (14)$$

The inlet and out pressures of the heat exchangers were calculated from the relative pressure losses given by:

$$P_{out} = P_{in}(1 - \Delta P) \quad (15)$$

Reactor Model: The reactor was modelled as a heat source supplying reactor thermal power at a specified temperature and efficiency. The heat gained is given by:

$$Q_g = W(C_{P_{out}} T_{out} - C_{P_{in}} T_{in}) \quad (16)$$

The heat source pressure loss is calculated in a similar way as shown in Eq. (15). The power plant thermodynamic states of temperature and pressure at all components were obtained by solving Eqs. (3) – (16)

Cycle Performance Calculation: The overall plant cycle assessment is represented as shaft output power (SOP), specific output power (SP), and cycle thermal efficiency. These are given by the following equations:

$$SOP = TW - CW/\eta_m \quad (17)$$

The capacity of the plant is represented as specific power (SP), given by:

$$SP = SOP/W \quad (18)$$

The cycle thermal efficiency (%) is given by:

$$\eta_{th} = SOP/Q_g \quad (19)$$

Component Matching: Component matching refers to the interactions between the gas turbine components which satisfies the engine matching conditions of mass and energy conservation to produce the system operating line. To be able to predict an accurate design and off-design point performance of the closed-cycle gas turbine would require matching of both the turbomachinery and heat exchangers. The following relationships in equations (20) – (26) are realized in order to obtain maximum matching in the recuperated closed-cycle system shown in fig.1.The matching process is comprehensively discussed in references [19,20,23]

$$\frac{W_T\sqrt{T_6}}{P_6} = \frac{W_c\sqrt{T_2}}{P_2} \times \frac{P_2}{P_3} \times \frac{P_3}{P_6} \times \sqrt{\frac{T_6}{T_2}} \times \frac{W_T}{W_c} \tag{20}$$

$$\frac{N_6}{\sqrt{T_6}} = \frac{N_2}{\sqrt{T_2}} \times \sqrt{\frac{T_2}{T_6}} \tag{21}$$

$$\frac{T_6 - T_7}{T_6} = \frac{T_3 - T_2}{T_2} \times \frac{T_6 - T_7}{T_3 - T_2} \times \frac{T_2}{T_6} \tag{22}$$

$$\frac{P_7}{P_6} \times \frac{P_2}{P_7} = \frac{P_2}{P_3} \times \frac{P_3}{P_6} \tag{23}$$

Map Scaling: The maps for different components were obtained using multi-fluid scaling methods which multiplies scaling factors derived at design point to the original component map at the off-design point. The following equations were used to obtain the scaling factor for off-design assessment.
The Corrected Mass Flow Scaling Factor (CMSF) is given as:

$$CMSF = \frac{(CMF_{cs})_{DP}}{\left(CMF_{map}\right)_{DP}} \tag{24}$$

Where,

$$CMF = \left(\frac{W\sqrt{\theta}}{\delta} \times \sqrt{\frac{R}{\gamma}}\right)$$

Similarly, the Pressure ratio Scaling Factor (PRSF) is obtained as:

$$PRSF = \frac{(PR_{DP} - 1)}{\left(PR_{DPmap} - 1\right)} \tag{25}$$

Component efficiency scaling factor is given by:

$$\eta_c SF = \frac{(\eta_c)_{DP}}{(\eta_c)_{DPmap}} \tag{26}$$

The iterative procedure for each control strategy is described in Fig (2) – (4). During off-design mode, the component geometry is held fixed from the design point case, and the shaft rotational speed, gas inventory, heat source and inlet temperature are varied to evaluate the performance of the power plant. This procedure utilizes the design point performance data to produce some input data for the off-design calculation. During the simulation analysis, the selected control options were assumed to operate independently at the same power level and the cooling medium was assumed to operate at constant temperature and flow.

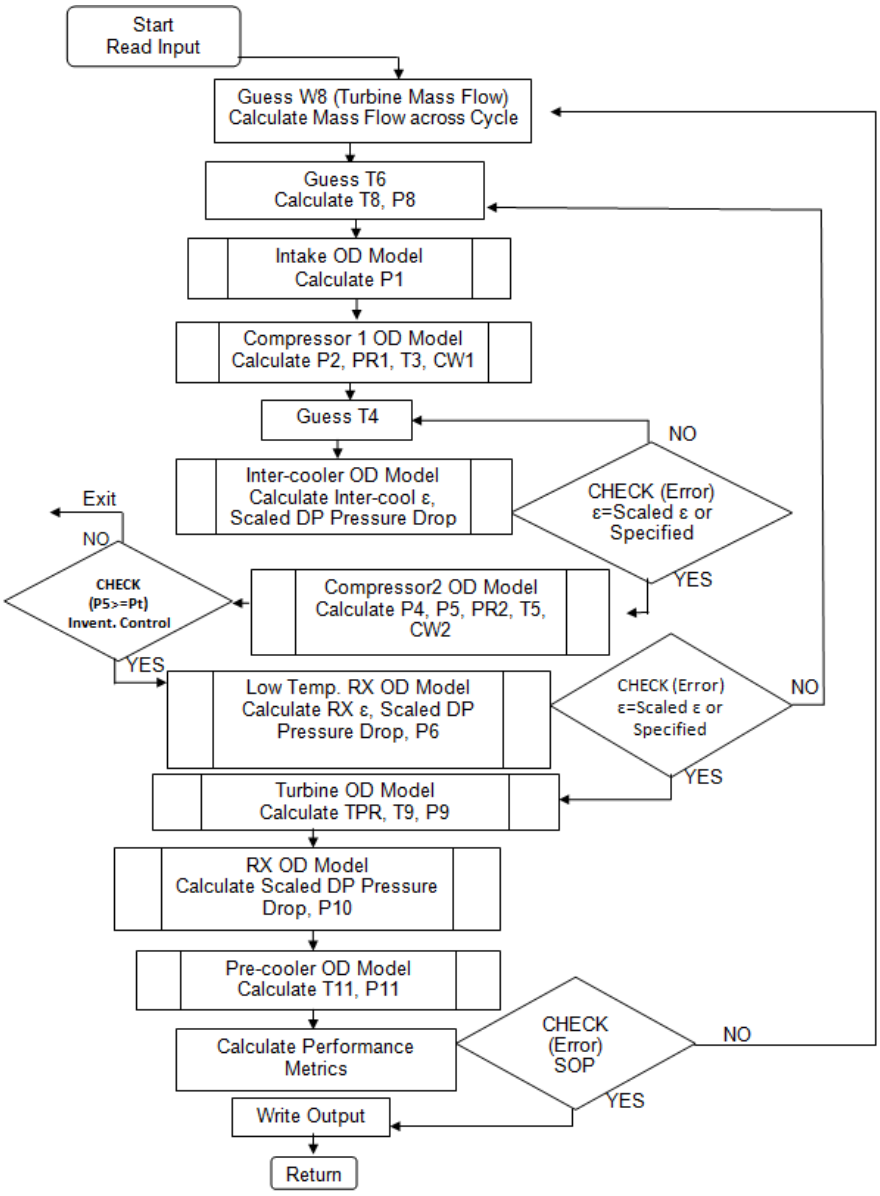

Figure 2: Iterative Procedure for Off-design Cycle using Inventory Control Strategy

Fig. 2 shows the iteration modelling procedure using inventory control at a steady-state condition. The iteration process starts with an initial guess of the turbine mass flow required to meet the part load demand. A modified Bitsch et al. [15]., model was implemented in an in-house simulation tool to develop a physical procedure to represent the inventory load control limit.

Minimum equilibrium inventory – control power range

$$\Omega_{min} = \frac{1 + \frac{M_{T1}}{M_{GT5}}}{1 + \psi\left(\frac{M_{T1}}{M_{GT5}}\right)} \tag{27}$$

For multi ICT option, where n > 1, then

$$\Omega_{min} = \Omega_{min}^{\frac{1}{n}} \tag{28}$$

Where the number of inventory tank is represented as n

The maximum equilibrium inventory – control power range is given by

$$\Omega_{max} = \frac{1 + \frac{M_{T1}}{M_{GT5}}}{1 + \left(\frac{\psi}{OPR}\right)\left(\frac{M_{T1}}{M_{GT5}}\right)} \tag{29}$$

Where

$$\psi = \frac{P_5}{P_{T1}} \tag{30}$$

$$n = number\ of\ storage\ tank$$

$$OPR = overall\ cycle\ pressure\ ratio$$

To model the thermodynamic behaviour of the plant utilising inventory control, the law of conservation of mass, conservation of momentum and conservation of energy was used to balance the fluid extraction and injection in the GT-cycle and storage tank relationship [24].

$$change\ in\ mass\ of\ tank \Delta M_T(kg) = \Delta M_{GT}\ (kg) \tag{31}$$

Where

$$\Delta M_T = \frac{\Delta P_T \times V_T}{RT_t} = \frac{\Delta P_{GT} \times V_{GT}}{RT_{GT}} = \Delta M_{GT} \tag{32}$$

Energy balance is given by

$$\delta Q - \delta W = \delta U + \delta PE + \delta KE \tag{33}$$

$$\delta W = 0, \delta KE = 0, \delta PE = 0$$

Where KE is the kinectic energy, PE is the potential energy, U is the internal energy

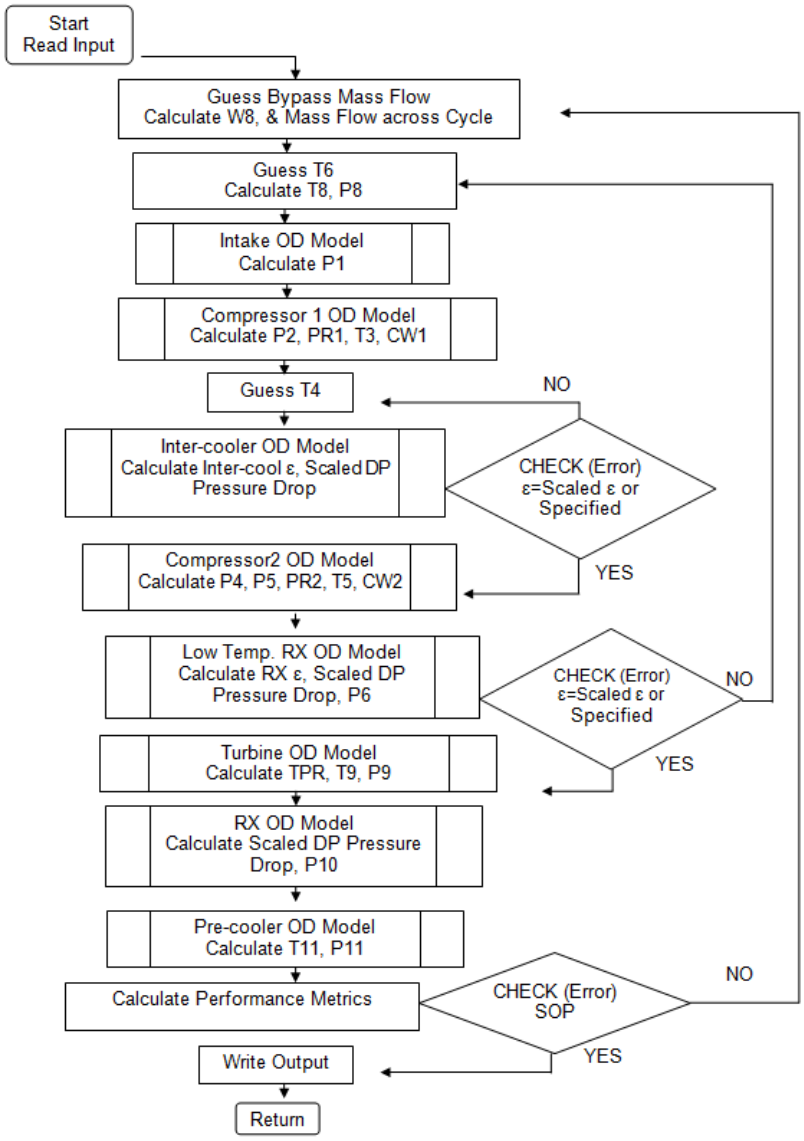

Figure 3: Iterative Procedure for Off-design Cycle using Bypass Control Strategy

Figure 3 shows the iterative procedure for bypass control. Similar to the inventory control, the mass flow is the regulating parameter. However, in this case, there is no interaction with the inventory tank. To this end, the model starts with an initial guess of the bypass mass flow for which the equations converges giving a shaft output power equal to shielded grid load. The impact of BCS on the performance is readily calculated since the cycle temperature may be taken to remain fixed. The recuperator will process equal masses on both sides at all times, which means that the ideal design situation of $T_6 = T_9$ is maintained at part-load as shown in fig. 1. This is due to the fact that with constant T_8 and constant compressor pressure ratio, $T_6 = T_9$. A mixer is introduced to combine the hot gas stream the cold gas stream, which balances the system enthalpy, thus, yielding $T_6 = T_9$.

In the in-house simulation tool [19], to model for load rejection and emergency stop, bypass control was implemented in pseudo-transient mode.'

Thus,

$$I\frac{d\omega}{dt} = G_t - (G_{cT} + G_L) \tag{34}$$

Where,

I = moment of inertia

G_t = Turbine torque

G_{cT} = total compressor torque

G_L= Load

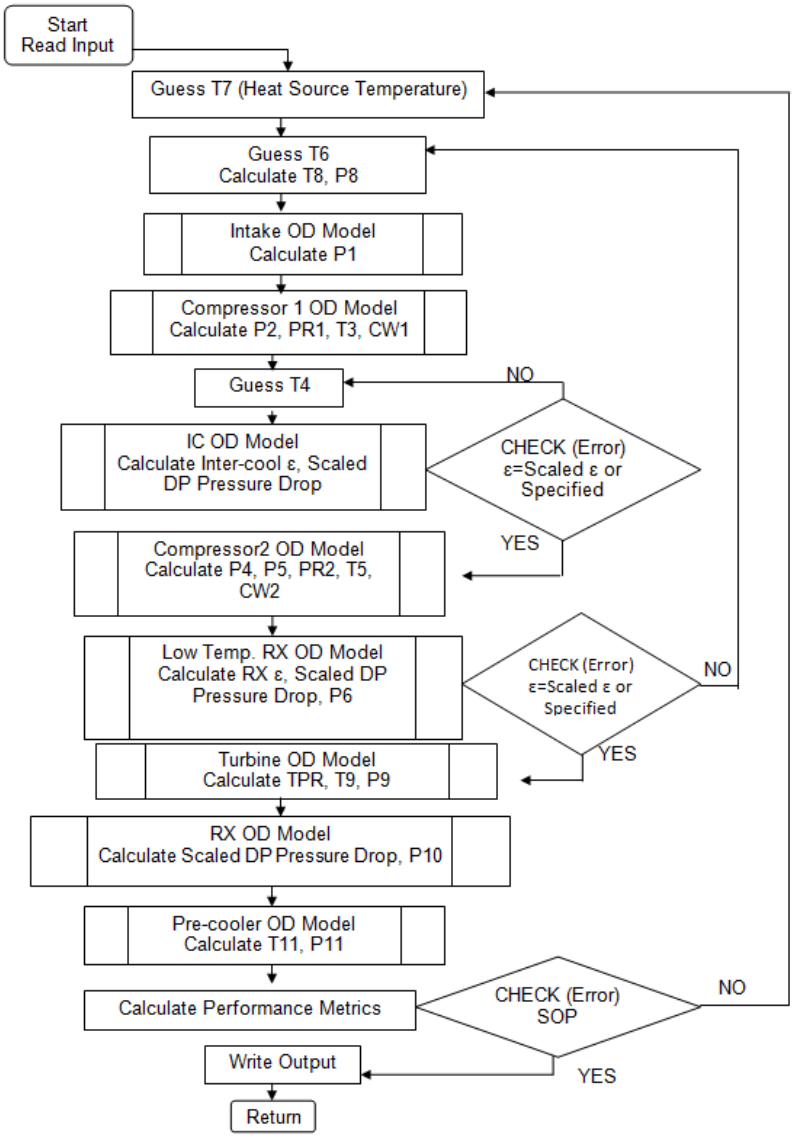

Figure 4: Iterative Procedure for Off-design Cycle using HST Control Strategy

Figure 4 describes the iterative procedure for HST control strategy. In this case, the initial guess is the reactor discharge temperature. The model uses the guess to calculate the non-dimensional parameter and matching of the GT components until the difference between the predicted shaft output and the actual load demand is less than or equal to 10^{-5}.

5. Results and Discussion

Generally, the primary goal of part-load operations using any control option is to maintain high efficiencies while keeping all components within their operating range. Theoretically, to achieve this will mean that overall temperature ratio and pressure ratio will be close to the steady state limits. However, this may not be easily satisfied using a single control option without making a compromise to certain practical constraints which are discussed in this analysis. In this study, an intercooled-recuperated closed cycle gas turbine shown in fig.1 and Table 1 was simulated using the selected control options discussed in this paper.

A – Cycle Performance at Part Load

Fig. (5) and (6) provides the part-load performance of the reference plant accomplished with the listed control strategies described in the preceding section. Each control option operates independently at the same power level. During the operation mode of the ICS, the mass of air is withdrawn from the power cycle almost proportional to the power output to keep the turbine entry temperature constant, whilst all temperature across the cycle remains constant for same LPC inlet conditions, which is controlled by the cooling medium. This withdrawal of mass flow reduces the density and pressures across the cycle. However, the pressure ratios of LPC and HPC remains constant because, the operating point $\frac{N}{\sqrt{T}}$ and the non-dimensional mass flow does not change significantly, hence, the cycle efficiency remains relatively constant as shown in figure 5. At 50% output power, the cycle thermal efficiency is 40.1%. The slight drop in efficiency is a result of a small change in the working fluid properties. Nonetheless, this control option brings about a rapid acceleration of the shaft as the load is reduced which must be balanced.

With the ICS, it seems that the possibility to further operate at a lower at part-load will still be very beneficial economically since the efficiency is still reasonably high. However, the possibility of maintaining high part-load efficiency to any desired limit using the inventory control is restricted to the following: (a) the size and initial pressure of the tank, (b) centrifugal force on blade tip as a result of shaft rotational speed, (c) location of inventory valves in the cycle loop (d) availability of inventory transfer compressor, and (e) cost of implementing any of the listed options.

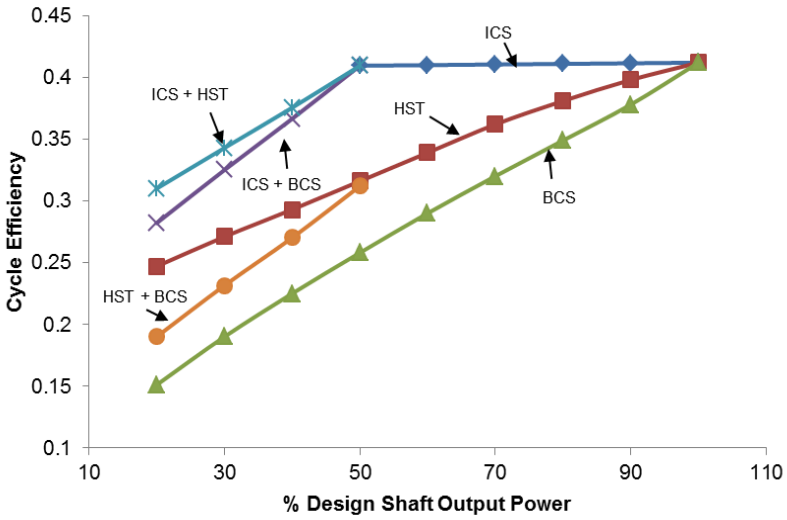

Figure 5 Cycle Efficiency for Different Control Strategy at Part Load

Similarly, when the bypass mode was analysed, ICS and HST were kept constant. The performance of the BCS is shown in Fig. 5 and Fig. 6. As mass flow is bled off after the HPC to short- circuit the turbine, there is relative mass flow difference between the compressor and turbine which is translated in the reduction of the HPC and turbine pressure ratios and mass density. This reduction modifies the operating point to a new position (the new matching point between the compressor and turbine) and reduces the turbine output power and cycle thermal efficiency as shown in Fig. 5 and Fig. 6. Both the LPC and HPC pressure ratio decreases with the dominant effect in the HPC. However, during this process, the LPC inlet pressure increases and the discharge pressure remain relatively the same at a steady state when the fluid returns to the circuit as shown in Fig.1. From the results presented, using BCS for 50% output power drops the cycle thermal efficiency to 25.8%. This control option can be an effective means of part-load control from zero to full load rejection. However, its major drawback is the low efficiency obtained compared with other control options.

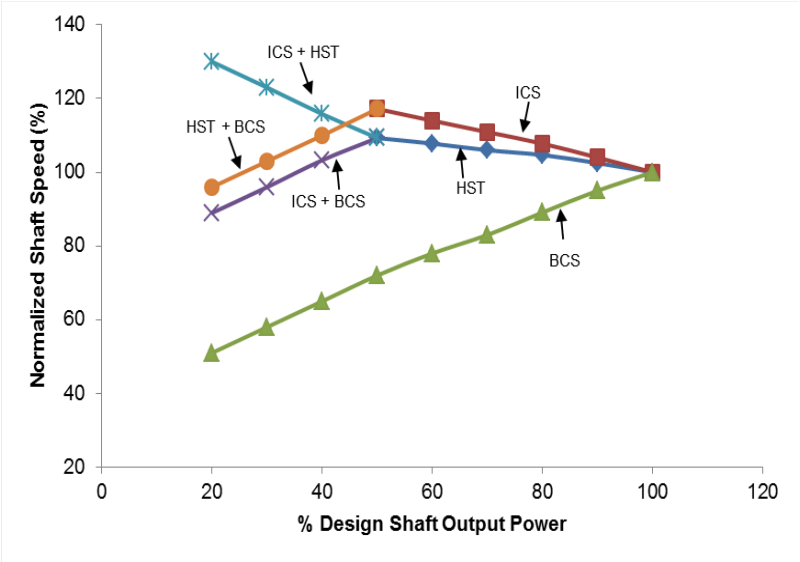

Figure 6 Shaft speed for Different Control Strategy at Part Load

Another way part-load operation can be achieved is by decreasing the cycle highest temperature which achieved via the heat source temperature control (HST). With HST in active mode, both the ICS and BCS are assumed to remain constant. At part-load operation, $\frac{T_8}{T_2}$ decreases as a result of a reduction in HST, and changes the position of the pressure ratios downward thereby reducing the cycle thermal efficiency almost linearly from 41.2% to 31% at 50% output power as shown in Fig. 5. During the process, as the TET decreases, the density of the fluid entering the turbine increases and thus decreases the volumetric flow rate (for the same mass flow rate), which decreases the turbine pressure ratio. To alleviate this will require the fluid inventory to be increased. One drawback of the control option is that decreasing the system temperatures will require a slow rate of change to avoid thermal shock.

Assuming some of the limitations mentioned for each control option are neglected, Fig 5 and Fig. 6 also shows performance comparison at part load in terms of overall cycle efficiency for each single control option and combination of two control options (second control option follows after the first control option). Simulating inventory followed by temperature control may not be feasible in practice without other control mechanisms since both strategies results to increase in shaft speed at part-load operations which could lead to mechanical failure of components. Inventory control followed by bypass is been mostly used for many closed-cycle power plant operations. This has been the most convenient method to stop the engine if required. Another realistic control measure is the temperature and bypass control.

B- Changes in Intake Temperature Condition

During this analysis, the intake inlet temperature was utilised as input. This was done as a representative of temperature to which the working gas is cooled before entering the compressor, which is dependent on ambient conditions, cooling medium and the design of the pre-cooler. Implementing the ICS during this off-design condition, showed that change in the LPC inlet temperature changes the temperature ratio, $N/\sqrt{T_1}$, and pressure ratio at constant HST. This changes result in a drop of shaft power and cycle thermal efficiency (Fig. 8) due to changes in the mass density. Hence, to compensate for this drop at constant power operation mode which is applicable to industrial power plant would require the opening of the ICS valves for injection of fluid. This injection causes an increase in mass flow and pressure in the circuit as shown in Fig. 7 and Fig. 8. Similarly, increased intake temperature reduces the LPC and HPC pressure ratios thereby resulting in a low expansion in the turbine and drop in output power. Therefore, HST control allows for an increase in turbine entry temperature, thereby increasing heat rate as shown in Fig. 9 and fig. 10

Apparently, implementing BCS for constant output power operation as intake temperature increases would require additional alternative control system because the mass flow has to be injected into the cycle which cannot be handled using the BCS alone.

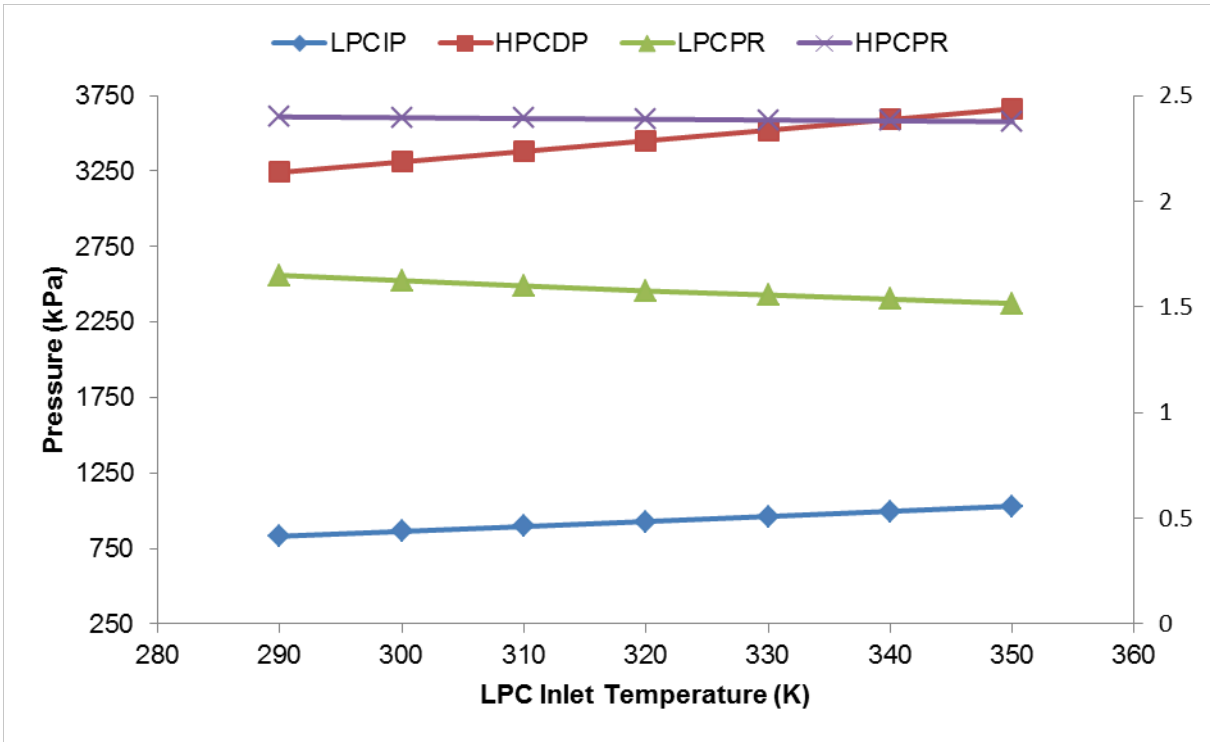

Figure 7: Effect of CIT on PR and Compressor Pressures using ICS

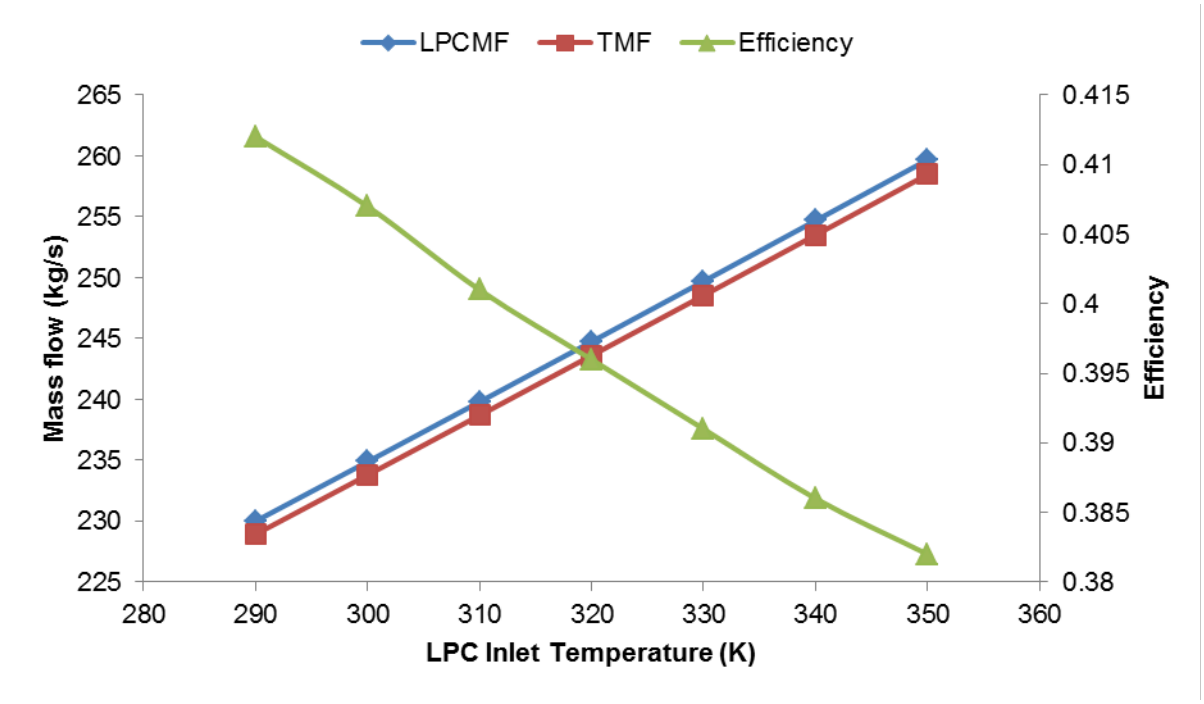

Figure 8: Effect of CIT on Mass Flow and Cycle Efficiency using ICS

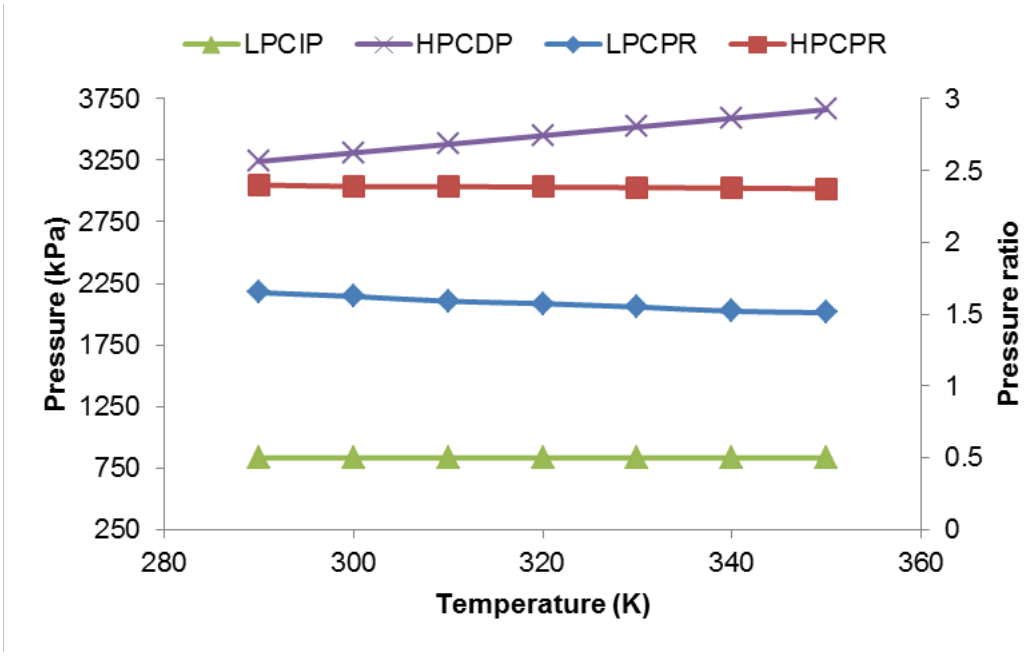

Figure 9: Effect of CIT on PR and Compressor Pressures using HST

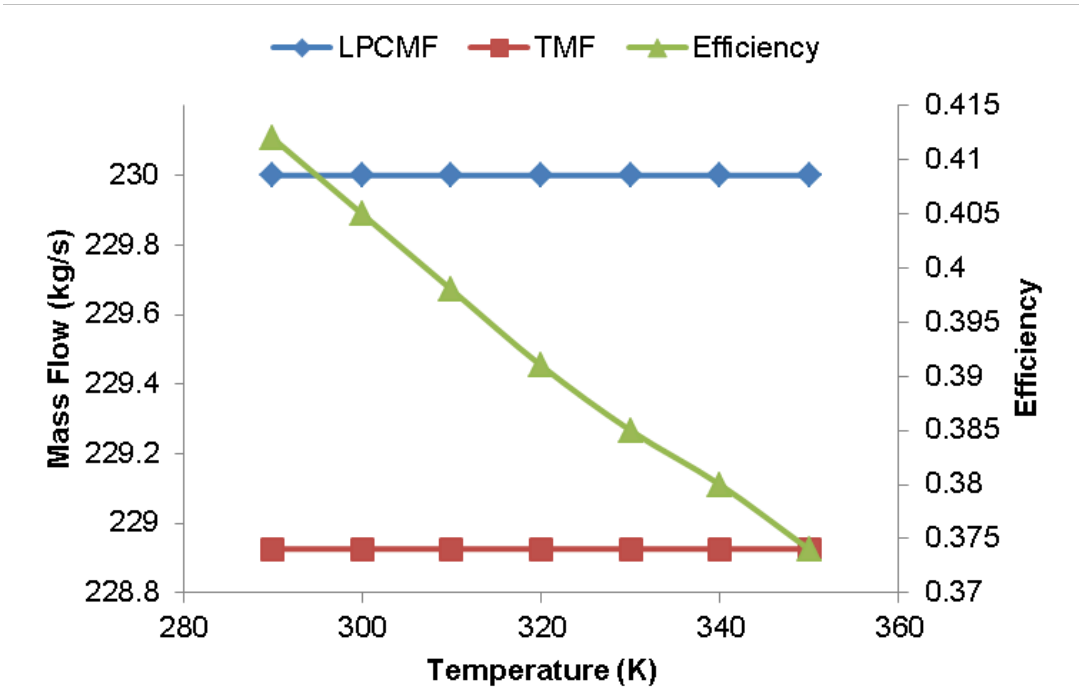

Figure 10: Effect of CIT on Mass Flow and Cycle Efficiency using HST

Comparing the performance result of the three control strategies discussed at both part-load and varying intake temperature shows that at 50% load demand, inventory control maintained a peak efficiency of 41.2%, while bypass control showed a rapid response to load change but produces the worst part load efficiency of 28% at same load demand. As changes in intake

temperature increases, bypass control cannot compensate for such a drop in power, hence would require another control mode to be activated. The results also showed that HST control yielded fairly high efficiencies at both operating conditions; however, further reduction at part load using HST or ICS could lead to mechanical failure of rotating parts [9,11,25]. Another impact on the mechanical integrity of the system will be on the seals and valves leakage at high temperature and pressure. Leakages in the system could lead to performance losses, hence, to minimise the losses could require proper sealing materials and external insulations.

C- **Load Rejection Control using BCS**

It is essential for the closed-cycle power plant to operate in an efficient, safe, secure and reliable manner, hence, the use of different control options. The goal of each control mechanism is to maintain a symbiotic relationship with load demand in the electric grid, especially during instabilities, interruptions and emergency conditions. Stability is maintained by matching the power generated with the ever-changing load demand which can be triggered by environmental conditions, load-following mode, load rejection or emergency stop.

Load following is being able to increase or decrease the power plant output to balance changes in load demand, which is usually achieved by controlling the inventory level. In contrast to load following, load rejection is defined as a very rapid decrease in load demand (usually when the rate of change of power output is >10%), which requires a rapid response via the control mechanism. Load rejection due to the loss of grid power is one of the most severe load control scenarios for the closed-cycle power plant which can be controlled with bypass valves (bypass valve rapidly opens to decrease the turbine work and increase compressor work to try to slow the accelerating shaft).

The focus of this section is to simulate load rejection mode using the bypass control mechanism for a power plant during operation. The following was assumed during the simulation of the load rejection:

- Only bypass control was utilized for this simulation
- Load rejection was simulated in steady-state pseudo transient operation (load rejections was set at 20% per seconds)
- The bypass valve size was assumed
- Rotor inertia was assumed
- Rotational speed was set at 3600rpm
- ICS and HST were kept constant
- Secondary effects were neglected

Figures (11) – (13) clearly shows the behaviour of the power plant during load rejection. In steady state operation of the plant, the torque developed must be balanced with the load torque determined by the required power. As the load torque changes, there is imbalance resulting in a change in the rotational speed, system temperatures and pressure ratios.

The bypass valve opens to prevent the turbomachine from over-speed and to keep the cycle operation ready for any load recovery. In reality, the bypass valve is designed to provide system shut down to an idle state as in the case of a load rejection, and completely stop as in the case

of any turbomachinery failure. However, during the process of bypass system control, other control processes are activated for example HST control to prevent thermal overstressing of the recuperators.

During the simulation, the steady state full power operation is disturbed with the load reduction starting at t = 0. The electric load is reduced at 20% per sec until 5 secs when it has reached the nominal no-load level. Fig 11, shows the reduction of the engine power output in case of a load release or quickly shut down within few seconds from 0% to 100% full load release by means of opening of the bypass valve and to maintain nominal engine speed. As can be seen, as the load release increases at BVC, the engine over-speed increases from 1% to 30% and the system pressure ratios also increase. The over-speed triggers the bypass valve to open. When the bypass valve is opened, the working fluid flow bypasses the turbine thereby reducing the turbine torque and power by reducing turbine flow and pressure ratio as shown in fig.11 & fig.12. This BVO results in a rise in temperature at the turbine output which is caused by a drop in expansion ratio and therefore the enthalpy gradient in the machine. Thus, the efficiency of the turbine reduces rapidly to almost zero percent at full load rejection. The precooler load increases as a major portion of the mass flow is circulated through it while the recuperator load decreases due to the low mass rate flowing through it as shown in fig 13.

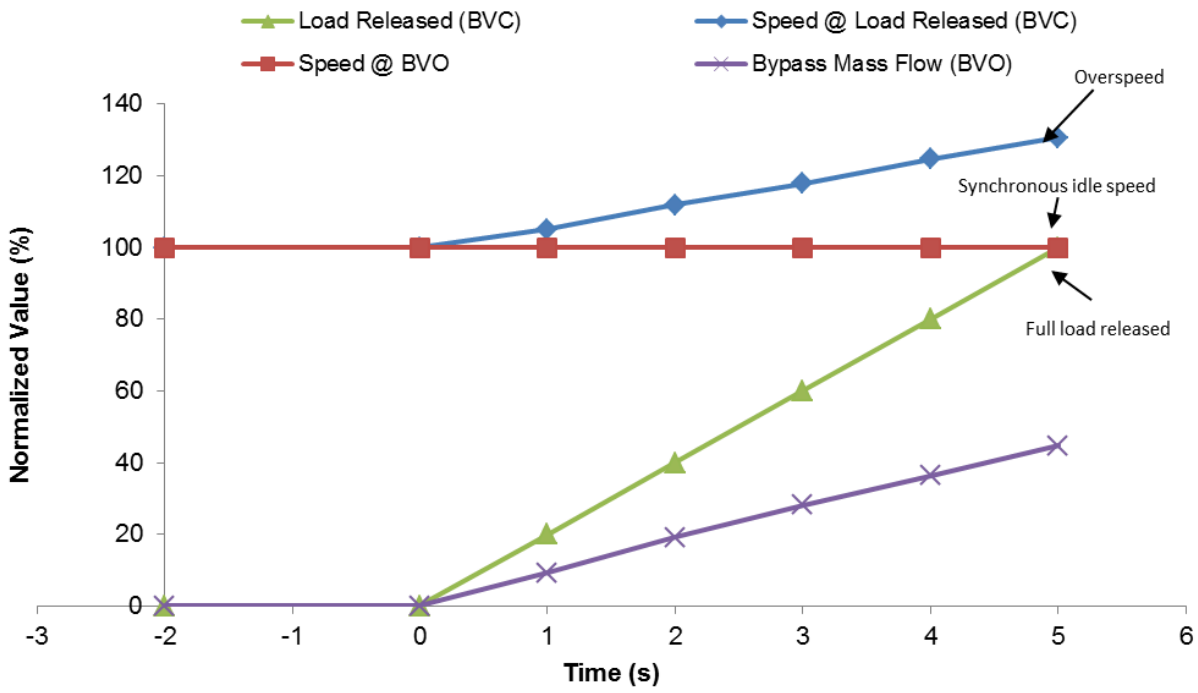

Figure 11 Estimation of Pseudo-Transient Behaviour with bypass control (speed & load released)

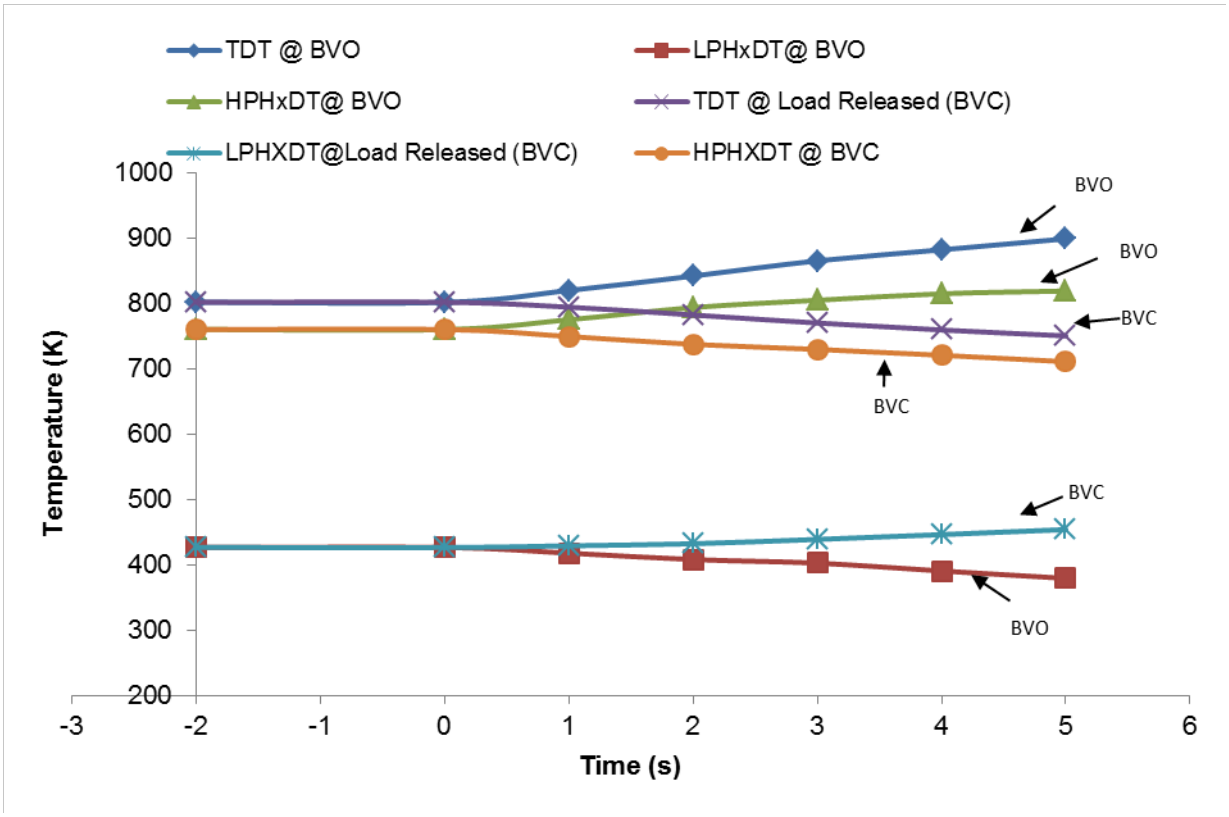

Figure 12 Estimation of Pseudo-Transient Behaviour with bypass control (system temperatures)

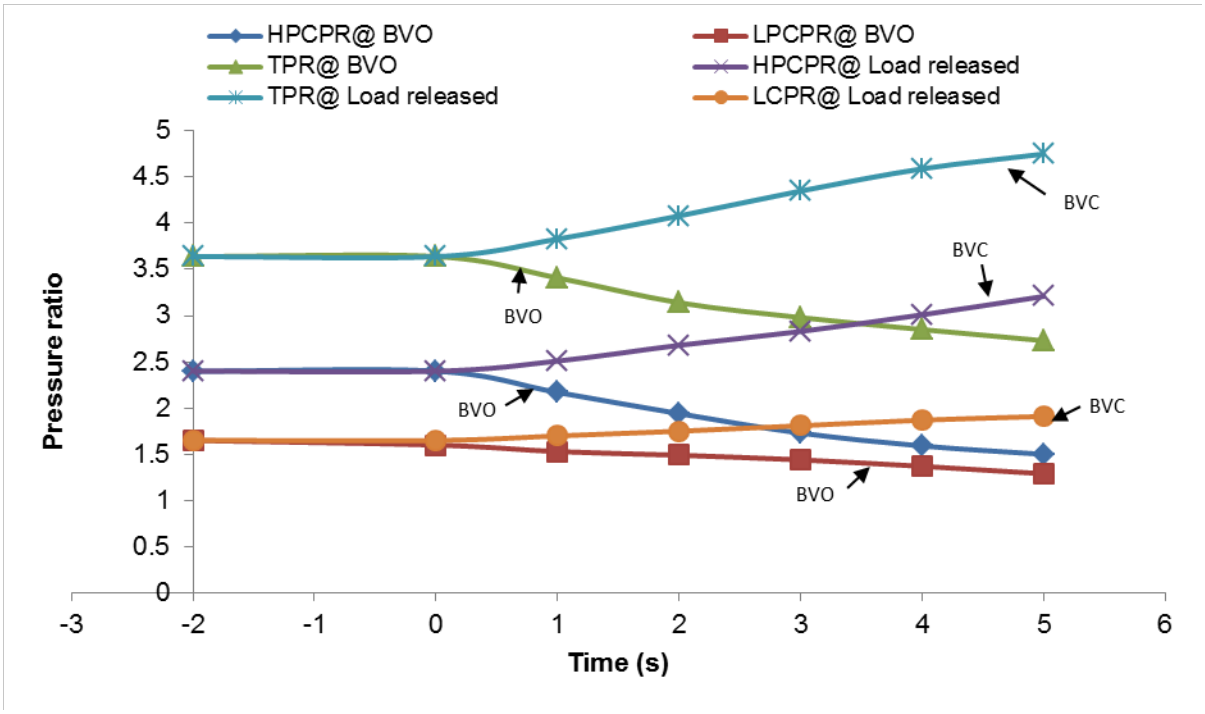

Figure 13 Estimation of Pseudo-Transient Behaviour with bypass control (system pressure ratios)

6. Conclusion

The performance of a single-shaft intercooled-recuperated closed-cycle gas turbine under three independent control strategies has been presented for part-load operation and load rejection. The rationale behind this analysis was to explore the different control strategy and its independent iterative procedure for a closed-cycle gas turbine, as well as to discuss the various limitations of the control options when used independently. The overarching discussions in this work can be concluded as follow:

- The iterative modelling procedure for each control strategy has been provided in order to enhance understanding of the control system during the closed-cycle gas turbine operation.
- The inventory control strategy has a high efficiency at both part-load and changes in ambient conditions compared with other control options presented in this paper. However, the continuous discharge of gas inventory from the gas turbine to achieve reduced load depends on the rotational speed for which the centrifugal forces acting on the blade tips could become too high, hence, could affect the mechanical integrity and compressor performance. Also, the size and pressure of the inventory tank is another limitation to the use of inventory control.
- Utilizing the heat source temperature is another important control strategy for the closed-cycle gas turbine operation. However, there is almost a linear decrease in cycle efficiency while operating at part load. On the other increasing the heat source temperature without the use of other control options in event of changes in ambient conditions could lead to shaft over speed.
- To operate in an efficient, safe, secure and reliable manner, each control mechanism is synchronised to maintain a symbiotic relationship with load demand or the electric grid, especially during instabilities, interruptions and emergency conditions. To avoid as much as possible these limitations in shaft speed or low efficiencies at a further reduction in power would require, a combined control mode to be adopted. For example, the bypass control usually implemented for rapid load response and shaft speed control.
- The possible leaks in the valve could lead to performance losses, hence, to minimise the losses, proper seal materials and external insulation could be incorporated.

Nomenclature

Notations

C	*heat capacity, J/K*
$\mathbf{C}^*$	heat capacity rate ratio, (nondimensional)
CMF	*corrected mass flow, kg/s*
CMSF	corrected mass flow scaling factor
C_P	*specific heat of gas at constant pressure, J/kg K*
CS	corrected speed
CW	*compressor work, W*
G_t	*turbine torque, J*
G_{ct}	*compressor torque, J*

G_L	*generator torque, J*
H	*specific enthalpy, J/kg*
I	*rotor inertia, kg m^2*
M_{GT}	*mass of fluid in gas turbine cycle, kg*
M_T	*mass of tank, kg*
N	*rotational speed, rpm*
NTU	number of transfer units
OPR	overall pressure ratio
P	*pressure, Pa*
P_{ref}	*reference pressure, Pa*
P_T	*inventory tank pressure, Pa*
PR	pressure ratio
PRSF	pressure ratio scaling factor
Q_g	*heat gained, W*
Q_{actual}	*actual heat flux, W/m^2*
Q_{max}	*maximum heat flux, W/m^2*
R	*specific gas constant, J/kg K*
SOP	*shaft output power, W*
SP	*specific power, W/kg s^{-1}*
T	*temperature, K*
T_{ref}	*reference temperature, K*
TDT	*turbine discharge temperature, K*
TET	*turbine entry temperature, K*
TMF	*turbine mass flow, kg/s*
TPR	turbine pressure ratio
TW	*turbine work, W*
W	*Mass flow rate, kg/s*
V_T	*volume of inventory tank, m^3*
V_{GT}	*volume of fluid in gas turbine cycle loop, m^3*

Greek Symbols

$\boldsymbol{\varepsilon}$	effectiveness
$\boldsymbol{\eta}$	efficiency
$\boldsymbol{\eta_m}$	mechanical efficiency
$\boldsymbol{\eta_{th}}$	cycle thermal efficiency
$\boldsymbol{\gamma}$	ratio of specific heats
$\boldsymbol{\theta}$	referred temperature parameter
$\boldsymbol{\delta}$	referred pressure parameter
$\boldsymbol{\Delta}$	difference
$\boldsymbol{\rho}$	density kg/m^3
$\boldsymbol{\Omega}$	inventory control level
$\boldsymbol{\psi}$	ratio of HPC exit pressure to tank pressure

Abbreviations

BCS	bypass control strategy
BVC	bypass valve close
BVO	bypass valve open
CIT	compressor inlet temperature
GH	*gas heater*
GT	*gas turbine*
HPC	*high pressure compressor*

HPCDP	high pressure compressor discharge pressure
HPCPR	high pressure compressor pressure ratio
HPHxDT	high pressure heat exchanger discharge temperature
HST	heat source temperature
IC	*inter-cooler*
ICR	*inter-cooled recuperator*
ICS	inventory control strategy
ICT	*inventory control tank*
ICV	*inventory control valve*
LPC	*low pressure compressor*
LPCIP	low pressure compressor inlet pressure
LPCMF	low pressure compressor mass flow
LPHxDT	low pressure heat exchanger discharge temperature
PC	*pre-cooler*
RX	*recuperator*
SF	*scaling factor*
VHTR	very high temperature reactor

Subscripts

c	*compressor*
c_{in}	*compressor inlet*
cold	*fluid cold stream*
c_{out}	*compressor outlet*
Dp	*design point*
Dprefmap	*design point reference map*
GT	*gas turbine cycle loop*
HEX	*heat exchanger*
hot	*fluid hot stream*
HPS	*high-pressure side*
in	*inlet condition*
LPS	*low-pressure side*
m	*mechanical*
max	*maximum*
min	*minimum*
OD	*off design point*
out	*outlet condition*
refmap	*reference map*
t	*turbine*
t_{in}	*turbine inlet*
t_{out}	*turbine outlet*
1-7	*station number*

References

1. Osigwe, E. O., 2018. Techno-economic and Risk Analysis of Closed-Cycle Gas Turbine Systems for Sustainable Energy Conversion, PhD Dissertation, Cranfield University, Cranfield, United Kingdom, 243 pages.
2. Osigwe, E. O., Gad-Briggs, A., Nikolaidis, T., Pilidis, P., Sampath, S., 2018. Performance Analysis of Generation IV Nuclear Reactor Power Plant Using CO_2 and N_2: Case Study of a Recuperated Brayton Gas Turbine Cycle. Proceedings of the ASME 2018 26th

International Conference on Nuclear Engineering, London, England, July 22-26, Paper No. ICONE26-81337, 8 pages.
3. Frutschi, H. U., 2005. Closed-Cycle Gas Turbines: Operating Experience and Future Potential, ASME Publishing, New York, USA, 283 pages.
4. Pradeepkumar, K. N., Tourlidakis, A., Pilidis, P., 2001. Analysis of a 115MW, 3- Shaft, Helium Brayton Cycle Using Nuclear Heat Source, Proceedings of ASME Turbo Expo: Power for Land, Sea, and Air, New Orleans, Louisiana, USA, June 4-7, 8 pages. Available at: doi:10.1115/2001-GT-0523
5. Covert, R. E., Krase, G., Morse, D. C., 1974. Effect of Various Contol Modes on the Steady-State Full and Part Load Performance of a Direct-Cycle Nuclear Gas Turbine Power Plant. Proceedings of ASME Winter Annual Meetings, New York, USA, November 17-22, 10 pages. Available at doi:10.1115/74-WA/GT-7
6. Gad-Briggs, A., Pilidis, P., Nikolaidis, T., 2017. Analyses of the Control System Strategies and Methodology for Part Power Control of the Simple and Intercooled Recuperated Brayton Helium Gas Turbine Cycles for Generation IV Nuclear Power Plants, ASME Journal of Nuclear Engineering and Radiation Science, Vol. 3, No. 4, 9 pages. Available at: doi:10.1115/1.4036737
7. Openshaw, F., Estrine, E., Croft, M., 1976. Control of a Gas Turbine HTGR, Proceedings of ASME Gas Turbine and Fluids Engineering Conference, New Orleans, USA, March 21-25, 12 pages.
8. Bammert, K., Krey, G., Krapp, R., 1974. Operation and Control of the 50-MW Closed-Cycle Helium Turbine Oberhausen, Proceedings of ASME International Gas Turbine Conference and Products Show, Zurich, Switzerland, March 30-April 4, 8 pages. Available at doi:10.1115/74-GT-13
9. Botha, B. W., Rousseau, P. G., 2006. Control options for Load Rejection in a Three-Shaft Closed Cycle Gas Turbine Power Plant, ASME Journal of Engineering Gas Turbines and Power, Vol. 129, No. 3, pp 806–813.
10. Bammert, K., Krey, G., 2010. Dynamic Behavior and Control of Single-Shaft Closed-Cycle Gas Turbines, ASME, Journal of Engineering Gas Turbines and Power, Vol. 93, No. 4, pp. 447–453. Available at doi:10.1115/1.3445605
11. Sanchez, D., Chacartegui, R., Munoz de Escalona, J. M., Sanchez, T., 2011. Performance Analysis of a MCFC & Supercritical Carbon Dioxide Hybrid Cycle under Part-Load Operation, International Journal of Hydrogen Energy, Vol. 36, No. 16, pp 10327–10336. Available at doi.org/10.1016/j.ijhydene.2010.09.072
12. Locatelli, G., Boarin, S., Pellegrino, F., Ricotti, M. E., 2015. Load following with Small Modular Reactors (SMR): A real options analysis, Energy, Vol. 80: pp 41–54. Available at: doi:10.1016/j.energy.2014.11.040
13. Singh, R., Kearney, M. P., Manzie C., 2013. Extremum-seeking Control of a Supercritical Carbon-dioxide Closed Brayton Cycle in a Direct-Heated Solar Thermal Power Plant, Energy, Vol. 60, pp 380–387. Available at: doi:10.1016/j.energy.2013.08.001
14. Gad-Briggs, A., Pilidis, P., Nikolaidis, T., 2017. Analyses of the Load Following Capabilities of Brayton Helium Gas Turbine Cycles for Generation IV Nuclear Power Plants, ASME Journal of Nuclear Engineering and Radiation Science, Vol. 3, No. 4, 8 pages. Available at: doi:10.1115/1.4036983
15. Bitsch, D., Chaboseau, J., 2015. Power Level Control of a Closed Loop gas Turbine by Natural Transfer of Gas between the Loop and Auxilliary Tanks, The British Nuclear Energy Society, 5 pages. Available at doi:10.1680%2Fngt.44678.0014
16. Osigwe, E. O., Obhuo, M., Pilidis, P., Sampath, S., Nikolaidis, T., 2018. Techno-Economic Study of Inventory Control Strategy for a Single-Shaft Intercooled-Recuperated Closed-Cycle Gas Turbine, Working Paper, Cranfield University.
17. Staudt, J. E., 1987. Design Study of An MGR Direct Brayton-Cycle Power Plant, PhD

Dissertation, Massachusetts Institute of Technology, Massachusetts, USA, 452 pages.
18. Yan, X., 1990. Dynamic Analysis and Control System Design for an Advanced Nuclear Gas Turbine Power Plant, PhD Dissertation, Massachusetts Institute of Technology, Massachusetts, USA, 392 pages.
19. Osigwe, E. O., Pilidis, P., Nikolaidis, T., Sampath, S., 2019. GT-ACYSS: Gas Turbine Arekret-Cycle Simulation Modelling for Training and Educational Purposes, ASME Journal of Nuclear Engineering and Radiation Science, 11 pages. doi:10.1115/1.4043681
20. Walsh, P. P., Fletcher, P., 1998. Gas Turbine Performance, Blackwell Science, Oxford, United Kingdom, 664 pages.
21. Shah, R. K., Sekulic, D., 2003. Fundamentals of Heat Exchanger Design, John Wiley & Sons, Inc., New Jersey, USA, 976 pages.
22. Kakac, S., Liu, H., 2002. Heat Exchangers Selection, Rating and Thermal Design, CPC Press, New York, USA, 520 pages.
23. Osigwe, E.O., Gad-Briggs, A., Nikolaidis, T., Pilidis, P., Sampath, S., 2018. Multi-Fluid Gas Turbine Components Scaling for a Generation IV Nuclear Power Plant Performance Simulation, Proceedings of the ASME 2018 26th International Conference on Nuclear Engineering, London, England, July 22-26, Paper No. ICONE26-82373, 8 pages.
24. Matimba, T. A. D., Krueger, D. L. W., Mathews, E. H., 2007. A Multi-tank Storage Facility to Effect Power Control in the PMBR Power Cycle, Nuclear Engineering and Design, Vol. 237, pp 153–160.
25. Munoz de Escalona, J. M., Sanchez, D., Chacartegui, R., Sanchez, T.,2013. Performance Analysis of Hybrid Systems Incorporating High-temperature Fuell cells and Closed Cycle Heat Engines at Part Load Operations, International Journal of Hydrogen Energy, Vol. 38: 570–578.

Performance modeling and analysis of a single-shaft closed-cycle gas turbine using different operational control strategy

Osigwe, Emmanuel O.

2019-07-18

Osigwe E, Gad-Briggs A, Igbong D, et al., (2020) Performance modeling and analysis of a single-shaft closed-cycle gas turbine using different operational control strategy. Journal of Nuclear Engineering and Radiation Science, Volume 6, Issue 2, April 2020, Article number 021201, Paper number NERS-19-1042

https://doi.org/10.1115/1.4044260